

## Article

# Optimal Design of Electric Vehicle Fast-Charging Station's Structure Using Metaheuristic Algorithms

Phiraphat Antarasee <sup>1</sup>, Suttichai Premrudeepreechacharn <sup>1</sup>, Apirat Siritaratiwat <sup>2</sup> and Sirote Khunkitti <sup>1,\*</sup> 

<sup>1</sup> Department of Electrical Engineering, Faculty of Engineering, Chiang Mai University, Chiang Mai 50200, Thailand

<sup>2</sup> Department of Electrical Engineering, Faculty of Engineering, Khon Kaen University, Khon Kaen 40002, Thailand

\* Correspondence: sirote.khunkitti@cmu.ac.th; Tel.: +66-868-589-799

**Abstract:** The fast development of electric vehicles (EVs) has resulted in several topics of research in this area, such as the development of a charging pricing strategy, charging control, location of the charging station, and the structure within the charging station. This paper proposes the optimal design of the structure of an EV fast-charging station (EVFCS) connected with a renewable energy source and battery energy storage systems (BESS) by using metaheuristic algorithms. The optimal design of this structure aims to find the number and power of chargers. Moreover, the renewable energy source and BESS can reduce the impact on the grid, so these energy sources are considered as ones of the optimally-designed structure of EVFCS in this work. Thus, it is necessary to determine the optimal sizing of the renewable energy source, BESS, and the grid power connected to EVFCS. This optimal structure can improve the profitability of the station. To solve the optimization problem, three metaheuristic algorithms, including particle swarm optimization (PSO), Salp swarm algorithm (SSA), and arithmetic optimization algorithm (AOA), are adopted. These algorithms aim to find the optimal structure which maximizes the profit of the EVFCS determined by its net present value (NPV), and the results obtained from these algorithms were compared. The results demonstrate that all considered algorithms could find the feasible solutions of the optimal design of the EVFCS structure where PSO provided the best NPV, followed by AOA and SSA.

**Keywords:** electric vehicle (EV); electric vehicle fast-charging station (EVFCS); renewable energy; particle swarm optimization (PSO); Salp swarm algorithm (SSA); arithmetic optimization algorithm (AOA)



**Citation:** Antarasee, P.; Premrudeepreechacharn, S.; Siritaratiwat, A.; Khunkitti, S. Optimal Design of Electric Vehicle Fast-Charging Station's Structure Using Metaheuristic Algorithms. *Sustainability* **2023**, *15*, 771. <https://doi.org/10.3390/su15010771>

Academic Editors: Seyed Masoud Mohseni-Bonab, Ali Moeini and Ali Hajebrahimi

Received: 25 November 2022  
Revised: 27 December 2022  
Accepted: 28 December 2022  
Published: 31 December 2022



**Copyright:** © 2022 by the authors. Licensee MDPI, Basel, Switzerland. This article is an open access article distributed under the terms and conditions of the Creative Commons Attribution (CC BY) license (<https://creativecommons.org/licenses/by/4.0/>).

## 1. Introduction

Nowadays, electric vehicles (EVs) play an important role in the automotive industry due to the use of fossil fuels and the environmental impacts of vehicles powered by internal combustion engines. For these reasons, the government and private sectors are coordinating attempts to reduce emissions of pollution and greenhouse gases. However, one of the most significant problems in promoting the popularity of EVs is the lack of EV charging stations (EVCS). In addition, EV customers can charge their EVs at home or work; however, the relatively long charging time may cause inconvenience in their use. Thus, it is necessary to install EV fast-charging stations (EVFCS) where EVs can be charged in less than 20 min in public, such as in parking lots [1,2]. On the other hand, the disadvantage to EVFCS is their high power usage, which can affect the grid. To solve this problem, renewable energy such as photovoltaic (PV), wind turbine (WT) and battery energy storage systems (BESS) must be installed in the EVFCS to mitigate the impacts on the grid. Moreover, when considering the design and development of EVFCS, one of the most important issues is to find the appropriate configuration of the EVFCS structure. This problem has resulted in various research about the optimal design of EVFCS or EVCS [2–11]. Over the past few decades, many proposals related to EVFCS or EVCS, including charging pricing strategies

or charging schedules, sizing and placing of the charging station, charging control, and design of EVCS or EVFCS structure have been investigated.

Several works have considered the problem of the optimal pricing strategy and the charging schedule of EVCS where different schemes or methods to minimize the charging cost have been presented. In [12], Zhang et al. proposed a pricing scheme to optimize charging scheduling for EVCS, which could minimize the service dropping rate of EVCS. The optimal charging schedule for EVs was presented by Savari et al. [13] to minimize the charging cost and charging time. The optimization algorithms, consisting of arrival time-based priority algorithm (ATP) and state of charge (SOC) based priority algorithm (SPB), were applied to solve the problem and compared with conventional algorithms, which are particle swarm optimization (PSO) and shuffled frog leaping algorithm (SFLA). Abbas et al. presented shifting peak hours demand to non-peak hours with a reduction in the average-to-peak ratio to minimize the charging cost and maximize the availability of charging capacity for EVs [14]. In [15], Hou et al. proposed varied charging pricing schemes to plan EV pathways by considering the charging fee, energy consumption, total time consumption, and driving distance. The charging pricing scheme was determined to maximize total revenues and balancing profits of EVCS by using PSO. The optimal charging scheduling scheme of EVs was introduced by Savari et al. [16] to reduce the charging cost by using PSO. Leou and Hung investigated the charging schedule of an electric bus charging station to determine the optimal contracted power capacity to minimize energy costs [17]. In [18], Shaaban et al. developed the online coordination approach for plug-in hybrid electric vehicles to minimize charging costs. This method aimed to optimally allocate the charging energy in low pricing periods to achieve minimum charging cost.

In addition, several methods to determine the optimal sizing and placing of the charging station have been proposed. In [1], Sadeghi-Barzani et al. used a mixed-integer non-linear programming (MINLP) approach by considering the station development cost, losses of EV energy and electric grid, as well as the placement of electric substations and urban roads, to find the optimal placing and sizing of the charging station. Second-order conic programming to formulate an optimization model by considering the time-varying nature of distributed generation and load consumption was proposed by Erdinc et al. [19]. This optimization model was adopted to obtain the optimal sizing and siting of various renewable resources-based DG units, charging stations, and energy storage systems within the distribution system. Hosseini and Sarder applied a Bayesian network (BN) model for handling risk assessment and decision-making to help address the uncertainty in charging station site selection that utilises economic, environmental, and social criteria (with a total of eleven sub-criteria) [20]. In [21], Hu et al. designed the optimal layout of the charging station by using a combined genetic algorithm with binary particle swarm optimization (GA-BPSO) to maximize the average number of covered EVs. Therefore, the problem of locating the charging station can be solved by using optimization algorithms. Furthermore, the control of the charging problem within EVCS has been designed and developed in a few works.

In the development of charging control, a few authors presented different charging control methods for solving the problem of the EVCS operation. In [22,23], Khalid et al. presented the topologies and charging control methods of advanced converters to reduce the oscillation in input supply, along with improving the energy flow between ESS and grid. The combined AC-DC model system, supported by a battery-swapping station, was proposed by Khalid et al. [24] to improve the issue of the power conversion and solve the limited distribution lines problem related to their thermal limit, due to the increasing power demand from EVs. Stojkovic analyzed the optimal charging control of EVs within EVCS powered by PV with 10 chargers [25]. This paper showed that such control could reduce the operational cost of EVCS and power losses in distribution feeders while meeting customer demands. In [26], Chen et al. designed the multiple-charger multiple-port charging (MCMP) system to provide the scheduling of a constrained number of chargers to accommodate a greater number of EVs. Savio et al. developed the converter control of multiport EV

charging to reduce the charging time because this controller provided constant current and voltage by closed-loop charging [27]. A few works which were mentioned above proposed the development of charging control; however, one of the important problems of EVFCS or EVCS development is to find the optimal design of structures within EVFCS or EVCS.

In the optimal designs of EVFCS or EVCS, many methods have been proposed and applied to optimize the designs of EVFCS or EVCS and operation. Some authors attempted to solve the optimal placement problem of EVFCS or EVCS by using different metaheuristic algorithms. In [3], Ahmad et al. proposed the optimal placing of the solar-powered charging station in the IEEE 33-bus system. Chicken swarm optimization (CSO), teaching-learning-based optimization (TLBO) and Java algorithms were applied to optimally place the charging stations with multi-objective problems by considering improved voltage profile, minimum power loss, and reduced cost as the objective functions. The multi-objective function maximizing voltage stability index, minimizing active and reactive power losses and average voltage deviation index were considered by Tounsi Fokui et al. [4] to optimize the placement of EVCS in the IEEE 69-bus system. A hybrid bacterial foraging optimization algorithm and PSO (BFOA-PSO) technique were proposed to solve this problem. Yenchanchalit et al. applied the cuckoo search algorithm (CSA), genetic algorithm (GA), and simulated annealing algorithm (SAA) to optimize the sizing of the installed PV within EVFCS and the position of EVFCS in the IEEE 33-bus system [5].

In addition, different metaheuristic algorithms have been presented in many works to optimize the structures such as the number and power of chargers, sizing of renewable energy sources and BESS, and operations of EVFCS or EVCS. The stand-alone electric tuk-tuk charging station in the Democratic Republic of Congo was designed by Vermaak and Kusakana [6] where the charging station was powered by energy from wind, PV, and BESS. HOMER software was applied to select the best configuration of those structures to maximize the total net present cost. Hafez and Bhattacharya introduced the optimal design of EVCS by considering the minimization of the lifecycle cost as the objective by using HOMER software [7]. The optimal energy storage system (ESS) size in EVFCS was proposed by Hussain et al. [8] to minimize the ESS cost and ensure the resilience of EVs during power outages. In [9], Dai et al. used the multi-agent particle swarm optimization algorithm (MAPSO) to find the optimal sizing of PV and BESS and determine the charging and discharging pattern of BESS and electric exchange with the grid. The results showed that the optimal sizing of the structures and operation could minimize the electricity cost. The optimal configuration of PV and battery, and the optimal design of operation for EVCS by using improved hybrid optimization genetic algorithm (iHOGA) software version 2.4, were examined by Badea et al. [10]. This software was applied to design PV and battery sizing to ensure that EVCS could accommodate EVs throughout all 24 h of the day in order to maximize the net present cost. In [11], Bhatti et al. computed the minimum numbers of PV modules and energy storage unit batteries for PV grid-connected charging systems by using PSO to decrease the charging price and impact on the grid. However, most of the papers about the design of EVFCS or EVCS have only focused on the problem of the placement or configuration structures within EVFCS or EVCS.

In [2], Domínguez-Navarro et al. presented the optimal design of EVFCS incorporating renewable energy sources and storage systems to maximize the profit measured by its net present value (NPV). GA was applied to find the structure of the EVFCS, consisting of the number and power of chargers, the number and type of wind generators, the installed area of PV panels, the storage system capacity, and the maximum power of the grid connected to the station. This algorithm was also used to optimize the operation of EVFCS and find the best solution that maximizes the profit or the NPV. The simulation results provided by GA were compared to those of PSO. However, the GA algorithm used in this work is very traditional, although many new and efficient optimization algorithms have been proposed. In addition, this work used an Erlang B queueing model to model the EV demand by simulating the arrival time of each EV, and also for the EV queueing system. Applying this

method to model the EV demand is appropriate; however, using this method for the EV queueing system is too complex and unnecessary.

Consequently, this paper proposes the optimal design of the structure of EVFCS for maximizing NPV. The optimal structural design of the EVFCS aims to find the number and power of chargers, the installed area of the PV panel, the sizing of BESS, and the grid power connected to the EVFCS. Moreover, the EV queueing system in this work is simpler than the methods in [2]. By using this concept, when EV customers arrive at the station and the chargers are unavailable, customers then immediately leave the station. To solve the optimization problem, three metaheuristic algorithms comprising PSO [28], Salp swarm algorithm (SSA) [29], and arithmetic optimization algorithm (AOA) [30] are employed. PSO is the traditional efficient algorithm which has been widely used to successfully solve many optimization problems [31–33]. SSA is a new algorithm which has efficiently solved several optimization problems in different fields [34–36]. Finally, AOA is a recently-proposed optimization algorithm which has been adopted to solve some optimization problems [37,38]. Thus, these algorithms are applied to find the optimal station's structure and used to manage the energy flow within the EVFCS, and their performance compared. The EVFCS can then achieve the maximum profit determined by its NPV, and solutions from these three algorithms are compared.

The main contributions of this work are as follows:

1. The optimal design of the EVFCS is investigated in order to maximize the NPV and optimize the energy flows in the EVFCS while the simple queueing method is used.
2. The optimal structure of the EVFCS consisting of the number and power of chargers, the installed area of PV panels, the BESS capacity, and the maximum grid power connected to the EVFCS is determined.
3. Three optimization algorithms including PSO, SSA, and AOA are applied to solve the design problem, and the solutions of these algorithms are compared.

The rest of the paper is divided as follows. Section 2 introduces the problem formulation of the optimal design of the EVFCS. Input data models used in this work are provided in Section 3. In Section 4, the formulations of the metaheuristic algorithms are given. Section 5 shows the simulation results together with comparison results. Finally, the conclusion of this work is presented.

## 2. Problem Formulation

The EVFCS considered in this work consist of many chargers to charge the batteries of the EVs. PV and BESS are also taken into account to increase profitability and reduce the impact on the grid. The design problem of the EVFCS is to find the optimal variables, the number and power of the chargers, the installed area of PV panels, the BESS capacity installed, and the maximum power of the grid connected to the EVFCS. This section defines the objective function and constraints of this work.

### 2.1. Objective Function

The objective function is to maximize NPV [2,6,7,9,10] formulated as the provided Equation (1):

$$NPV = \sum_{t=1}^n \frac{NCF_t}{(1+i)^t} - I \quad (1)$$

where  $NCF_t$  is the net cash flow (\$) at year  $t$ ,  $I$  is the investment cost (\$),  $i$  is the interest rate (%), and  $n$  is the time of the cash flow considered (year). The  $NCF_t$  at each year  $t$  can be calculated as following Equation (2):

$$NCF_t = \sum_{h=1}^{8760} (INFLOW_h - OUTFLOW_h) - Cr_t - Cm_t - Cgrid_t \quad (2)$$

where  $INFLOW_h$  is the cash inflows (\$) at an hour  $h$ ,  $OUTFLOW_h$  is the cash outflows (\$) at an hour  $h$ ,  $Cr_t$  is the cost of replacing BESS (\$) at year  $t$ ,  $Cm_t$  is the cost of maintaining BESS (\$) at year  $t$  which is equal to \$1181.10/year [2] in this work, and  $Cgrid_t$  denotes the cost of contracting power to the grid (\$) at year  $t$ . The  $INFLOW_h$  and  $OUTFLOW_h$  can be computed as provided Equations (3) and (4):

$$INFLOW_h = Eev_h \times Cs + Es2g_h \times Csale \quad (3)$$

$$OUTFLOW_h = Eg2s_h \times Cbuy \quad (4)$$

where  $Eev_h$ ,  $Es2g_h$  and  $Eg2s_h$  are the energy charged to EVs (kWh), the energy sold to the grid (kWh) and the energy purchased from the grid (kWh) at an hour  $h$ , respectively, and  $Cs$ ,  $Csale$ , and  $Cbuy$  are the sale price of energy to EV (\$/kWh), the sale price of energy to the grid (\$/kWh), and the buy price of energy from the grid (\$/kWh), respectively. The  $Cr_t$  and  $Cgrid_t$  are formulated as Equations (5) and (6) below:

$$Cr_t = \frac{\sum_{h=1}^{8760} EDsto_h}{ETVsto} \times Csto \times Esto_{inst} \quad (5)$$

$$Cgrid_t = Cgc_m \times Pgc_{max} \quad (6)$$

where  $EDsto_h$  is the energy discharged from BESS (kWh) at an hour  $h$ ,  $ETVsto$  is the life cycle by battery capacity (kWh) or its volume of total energy,  $Esto_{inst}$  is the BESS capacity installed (kWh),  $Csto$  is the cost of BESS (\$/kWh),  $Cm_t$  is the cost of BESS maintaining at year  $t$ ,  $Cgc_m$  is the cost of contracting power to the grid (\$) at the mount  $m$ , and  $Pgc_{max}$  is the maximum grid power connected to the EVFCS (kW). The investment cost from (1) is calculated as Equation (7):

$$I = Cch \times Qch \times Pch_{inst} + Cpv \times Apv_{inst} + Csto \times Esto_{inst} \quad (7)$$

where  $Pch_{inst}$  is the power of the chargers installed (kW),  $Apv_{inst}$  is the area installed of PV panels ( $m^2$ ),  $Cch$  and  $Cpv$  are the cost of the charger (\$) and the cost of PV panels (\$/ $m^2$ ), and  $Qch$  is the number of chargers installed.

## 2.2. Constraints

Various constraints must be considered while solving the optimization problem. The constraints of the considered problem comprise the energy balance within the EVFCS, limit of BESS, limits of the installed PV, and limit of the power exchange between the grid and EVFCS [2].

### 2.2.1. Equality Constraints

#### 1. Energy balance:

The energy balance at each hour in the EVFCS must be equal to zero. In each hour  $h$ , the summation of the energy generated from PV, the energy purchased from the grid, and the energy discharged from BESS must be equal to the summation of the energy charged to EVs, the energy sold to the grid and the energy charged to BESS. So, the energy balance is formulated as given Equation (8):

$$Eph_h + Eg2s_h + EDsto_h = Eev_h + Es2g_h + ECsto_h \quad (8)$$

where  $Esoc_h$  and  $Esoc_{h-1}$  are the SOC of BESS at an hour  $h$  and at an hour  $h - 1$ , respectively.

#### 2. State of charge (SOC) of BESS:

SOC of BESS at an hour  $h$  is equal to SOC of BESS at the previous hour  $h - 1$ , plus the charged energy at that hour  $h$ , minus the discharged energy at that hour  $h$ . SOC of BESS is shown in Equation (9) below:

$$Esoc_h = Esoc_{h-1} + ECsto_h - EDsto_h \quad (9)$$

where  $Esoc_h$  and  $Esoc_{h-1}$  are the SOC of BESS at an hour  $h$  and at an hour  $h - 1$ , respectively.

### 2.2.2. Inequality Constraints

#### 1. Limits of BESS:

The discharged energy by BESS at each hour  $h$  must be less than the SOC of BESS at the previous hour  $h - 1$ . The energy charged to BESS must be less than the installed BESS capacity minus SOC of BESS at the previous hour, as shown in Equations (10) and (11):

$$EDsto_h \leq Esoc_{h-1} \quad (10)$$

$$ECsto_h \leq Esto_{inst} - Esoc_{h-1} \quad (11)$$

#### 2. Limits of the stored energy in BESS:

The SOC of BESS at an hour  $h$  must be equal to or less than the installed BESS capacity and equal to or higher than its minimum SOC, as shown in Equations (12) and (13):

$$Esoc_h \leq Esto_{inst} \quad (12)$$

$$Esoc_h \geq SOC_{min} \times Esto_{inst} \quad (13)$$

where  $SOC_{min}$  is the minimum SOC of BESS capacity.

#### 3. Limits of BESS powers:

The power discharged and charged by BESS at each hour  $h$  must be less than the power of the installed BESS, as defined by Equations (14) and (15):

$$PDsto_h \leq Psto_{inst} \quad (14)$$

$$PCsto_h \leq Psto_{inst} \quad (15)$$

where  $PDsto_h$  and  $PCsto_h$  are the power discharged and charged by BESS at an hour  $h$ , respectively.

#### 4. Limit of the power generated by PV:

The power generated by PV at an hour  $h$  must be less than the power of the installed PV, defined in Equation (16):

$$Pph_h \leq Pph_{inst} \quad (16)$$

where  $Pph_h$  is the power generated by PV at an hour  $h$ , and  $Pph_{inst}$  is the power of the installed PV.

#### 5. Limits of the connected grid power to EVFCS:

The power purchased and sold at an hour  $h$  between the grid and EVFCS must be equal to or less than the maximum power of the connected grid to the station, as shown in Equations (17) and (18):

$$Ps2g_h \leq Pgc_{max} \quad (17)$$

$$Pg2s_h \leq Pgc_{max} \quad (18)$$

where  $Ps2g_h$  and  $Pg2s_h$  are the power purchased to the grid and sold from the grid at an hour  $h$ , respectively.



### 3. Input Data Models

In this section, the input data used to simulate the optimization problem consisting of EV demands, energy generated from PV, and BESS operation are explained as shown below.

#### 3.1. EV demands

The EV demands are initially modeled as the input data. This model is determined by the EV types and their battery capacities, the SOC level of the EV's battery, and the time that EVs arrive at the EVFCS.

In the first step, the types of EVs are classified according to the battery capacity of the EVs. This data was based on the registration of electric vehicle data obtained from the Traffic General Direction of Spain [2]. This data is used to provide discrete probability distributions of battery capacity for each type of EV that can be charged in the EVFCS, including motorcycles, cars, and vans. The discrete probability distributions of the battery capacity of EVs are shown in Table 1.

**Table 1.** Probability of EV's battery capacity.

Type	Battery Capacity (kWh)	Probability (%)	Accumulated Probability (%)
Motorcycle	3.6	0.115	0.115
Small car	16	0.370	0.485
Large car	25	0.380	0.865
Van	63	0.135	1.000

In the second step, the SOC of each EV's battery is simulated using the Lognormal Distribution [2,39] as shown in Equation (19):

$$SOC(E; \mu, \sigma) = \frac{1}{E\sigma\sqrt{2\pi}} \times e^{-(\ln E - \mu)^2 / 2\sigma^2} \quad (19)$$

where  $\mu$  and  $\sigma$  are the average and typical deviation values of the logarithm equation, respectively, and  $E$  is the initial SOC level in the EV's battery which is between 0 and 1. In this work,  $\mu$  and  $\sigma$  are 3 and 0.6, respectively [2].

In the model process, the battery capacity of EVs and EV type that arrives at the EVFCS are obtained by comparing the accumulated probability in Table 1 with a random number between 0 and 1. Another random number is also generated to give the random  $E$  value for each EV that arrives at the EVFCS to obtain the SOC level of the EV's battery.

Then, when the battery capacity and the SOC of each EV are obtained, these two values will be used to calculate the charging time [2] as in presented Equation (20):

$$Charging\ time = \frac{EV's\ battery\ capacity \times (1 - SOC)}{Pch_{inst}} \quad (20)$$

Finally, the time that EVs arrive at the EVFCS can be simulated by using Erlang B queueing method and Sequential Monte Carlo (SMC) [2]. In this work, the simulation results obtained from [2] are adopted to determine the electricity demands or loads of EVs by the time and number of EVs arriving at the EVFCS as presented in Figure 1.

#### 3.2. PV Energy and BESS

PV is considered in this work to reduce the usage energy from the grid, and it can also improve the profit of the EVFCS by selling the excess electricity to the grid. The hourly power generated by the PV panels can be calculated as given Equation (21) [2,6,40]:

$$Ppv_h = G_h \times Apv_{inst} \times \eta \quad (21)$$

where  $G_h$  is the hourly global solar irradiance at the PV panel ( $W/m^2$ ) at an hour  $h$ , and  $\eta$  is the system efficiency value, which is 17% [2] in this work.

$G_h$  is obtained from the Photovoltaic Geographical Information System (PVGIS) program [41], which calculates the total solar irradiance of the inclined panel of each area [2].

Lithium-ion (Li-ion) batteries [2,8,11,42,43] have been considered as the BESS [2,8,10,11,44,45] in this work, and the BESS operates under two conditions. In the first condition, the energy from PV is considered the first priority to feed the EVFCS. If the energy from PV is greater than the energy needed from the EVFCS, the excess energy will be stored in the BESS. When the BESS reaches its maximum capacity, the excess energy is then sold to the grid. In the other condition, once PV is unavailable or the energy generated from PV is less than the energy demand of the EVFCS, the BESS firstly feeds the energy to the EVFCS until the BESS's minimum capacity is reached. Buying energy from the grid is the last option. Aside from that, the calculated energy flows and management must be limited in the constraints as in (8)–(18) [2,9–11].

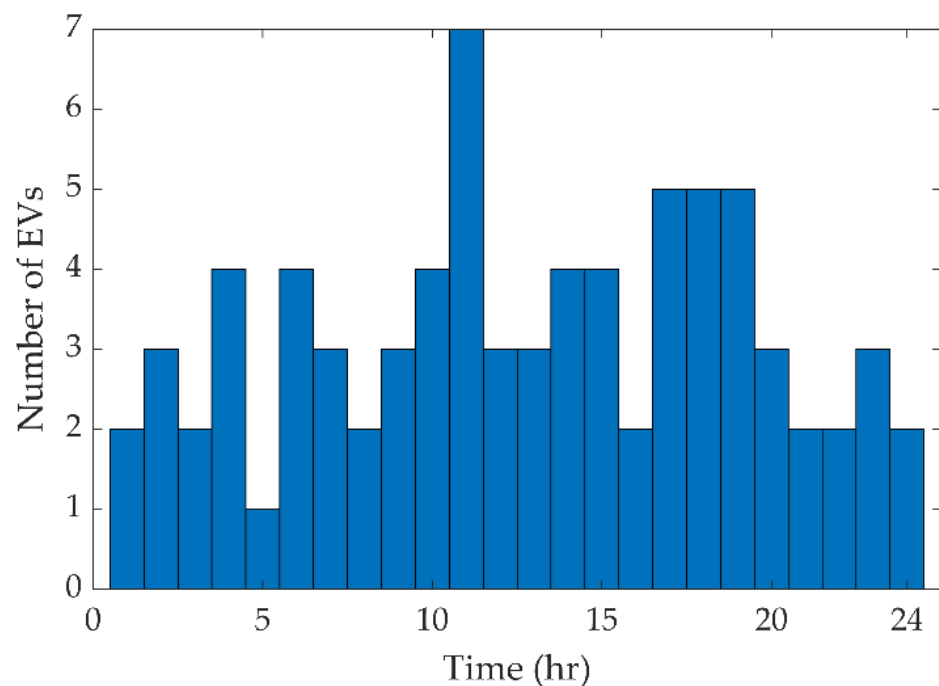


**Figure 1.** Number of EVs arriving at the EVFCS in each hour [2].

#### 4. Metaheuristic Algorithms

To solve the optimization problem, three metaheuristic algorithms consisting of PSO, SSA, and AOA are applied. The formulations of each algorithm are described in the following subsections.

##### 4.1. Particle Swarm Optimization (PSO)

PSO is a computational method to find the best solution of the optimization problem proposed by Kennedy and Eberhart in 1995 [28]. A fundamental concept derived from mimicking the foraging behavior of a flock of birds, each member of the flock will search for food by following the member which is the closest to the best food source at that moment. The PSO consists of particles that will constantly find the best solution, and each particle represents a possible solution. The velocity and position of each particle are modified in each iteration by using following Equations (22) and (23):

$$X_i(t+1) = X_i(t) + V_i(t+1) \quad (22)$$

$$V_i(t+1) = w(t) \times V_i(t) + c_1 \times rand(Pbest_i(t) - X_i(t)) + c_2 \times rand(Gbest(t) - X_i(t)) \quad (23)$$



where  $X_i(t)$  and  $V_i(t)$  are the position and velocity of a particle  $i$  at iteration  $t$ , respectively,  $X_i(t+1)$  and  $V_i(t+1)$  are the position and velocity of a particle  $i$  at iteration  $t+1$ ,  $Pbest_i(t)$  and  $Gbest_i(t)$  are the best position of the particle  $i$  (personal best) and the best position of the whole particle (global best) at iteration  $t$ , respectively,  $rand$  is a random value between 0 and 1,  $c_1$  and  $c_2$  are positive constant values which are both set to 2 in this work, and  $w(t)$  denotes the inertia weight at iteration  $t$ . The  $w(t)$  can be calculated as Equation (24) below:

$$w(t) = w_{max} - \frac{w_{max} - w_{min}}{Iter_{max}} \times Iter \quad (24)$$

where  $w_{max}$  and  $w_{min}$  are the maximum and minimum inertia weights which are set to 0.9 and 0.4 in this work, respectively,  $Iter_{max}$  is the maximum iteration, and  $Iter$  is the current iteration [46].

#### 4.2. Salp Swarm Algorithm (SSA)

SSA is an efficient population-based algorithm proposed by Mirjalili in 2017 [29]. SSA parodies the Salp swarm behavior during ocean foraging. Salps typically form a swarm called a Salp chain in dense waters where a Salp at the front of the chain is the leader and the rest of the Salps are followers. Each Salp represents the position in an  $x$ -dimensional search space where  $x$  is a vector of variables of an optimization problem. The leader Salp position can be updated by Equation (25) below:

$$x_j^1 = \begin{cases} F_j + c_1((UB_j - LB_j) \times c_2 + LB_j), & c_3 \leq 0 \\ F_j - c_1((UB_j - LB_j) \times c_2 + LB_j), & c_3 > 0 \end{cases} \quad (25)$$

where  $x_j^1$  and  $F_j$  denote the leader Salp position and the food source position in dimension  $j$ , respectively,  $UB_j$  and  $LB_j$  are the upper and lower bounds of each variable in dimension  $j$ , respectively, and  $c_1$ ,  $c_2$ , and  $c_3$  are random variables generated between 0 and 1 to preserve the search space,  $c_1$  is the major parameter as it helps to balance the capabilities of the exploration and exploitation phases.  $c_1$  can be calculated by presented Equation (26):

$$c_1 = 2 \times e^{-\left(\frac{4 \times Iter}{Iter_{max}}\right)^2} \quad (26)$$

When the leader Salp position is obtained, the next step is to update the positions of followers, which are calculated as given Equation (27):

$$x_j^i = \frac{1}{2}(x_j^i + x_j^{i-1}) \quad (27)$$

where  $x_j^i$  denotes the position of the follower  $i$  in dimension  $j$ , and  $i$  is greater than 1.

#### 4.3. Arithmetic Optimization Algorithm (AOA)

AOA is the population-based algorithm proposed by Abualigah in 2021 [30]. In the process of AOA, the simple arithmetic operators (Subtraction (S), Addition (A), Division (D), and Multiplication (M)) are used to optimize and determine the best solutions.

The first step of the AOA is to randomly create a candidate solution ( $X$ ) in each iteration. The best candidate solution is supposed to be the optimum solution so far.  $X$  can be formulated as shown in Equation (28):

$$X = \begin{bmatrix} x_{1,1} & \cdots & x_{1,j} & x_{1,n-1} & x_{1,n} \\ x_{2,1} & \cdots & x_{2,j} & \cdots & x_{2,n} \\ \cdots & \ddots & \vdots & \ddots & \vdots \\ x_{N-1,1} & \cdots & x_{N-1,j} & \vdots & x_{N-1,n} \\ x_{N,1} & \cdots & x_{N,j} & x_{N,n-1} & x_{N,n} \end{bmatrix} \quad (28)$$

Then, the algorithm calculates the math optimizer accelerated (*MOA*) function which is used to select the search phase. *MOA* function value at each iteration is a coefficient calculated by following Equation (29):

$$MOA(Iter) = Min + Iter \times \left( \frac{Max - Min}{Iter_{max}} \right) \quad (29)$$

where *Min* and *Max* are the minimum and maximum values of the accelerated function, respectively.

The simulation of the behaviors of Arithmetic operators has been operated by the simple rule. For the exploration phase, the position is updated by provided Equation (30):

$$x_{i,j}(Iter + 1) = \begin{cases} x_{best,j} \div (MOP + \varepsilon) \times ((UB_j - LB_j) \times \mu + LB_j), & r_2 < 0.5 \\ x_{best,j} \times MOP \times ((UB_j - LB_j) \times \mu + LB_j), & otherwise \end{cases} \quad (30)$$

where  $x_{i,j}(Iter + 1)$  is the position  $j$  of the solution  $i$  at iteration  $Iter + 1$ ,  $x_{i,j}(Iter)$  is the position  $j$  of solution  $i$  at iteration  $Iter$ ,  $x_{best,j}$  denotes the best-obtained solution of position  $j$ , and  $\varepsilon$  indicates a small integer number.  $UB_j$  and  $LB_j$  are the upper and lower bounds of position  $j$ , respectively, and  $\mu$  indicates the control parameter to adapt the search process, which is 0.5 in this work. *MOP* is the math optimized probability calculated by following Equation (31):

$$MOP(Iter) = 1 - \frac{Iter^{1/\alpha}}{Iter_{max}^{1/\alpha}} \quad (31)$$

where  $\alpha$  indicates a sensitive parameter and defines the exploitation accuracy over the iterations which is equal to 5 in this work.

In the exploitation phase, the AOA is operated by executing Subtraction (S) and Addition (A) which is conditioned by *MOA* value for the condition of  $r_1$  is not greater than *MOA* value. The exploitation operators (S and A) of AOA explore the search space in depth on various intensive regions and both operators' search techniques are used to find a better solution, which is modeled as given Equation (32):

$$x_{i,j}(Iter + 1) = \begin{cases} x_{best,j} - MOP \times ((UB_j - LB_j) \times \mu + LB_j), & r_3 < 0.5 \\ x_{best,j} + MOP \times ((UB_j - LB_j) \times \mu + LB_j), & otherwise \end{cases} \quad (32)$$

#### 4.4. Imprementation

The implementation of the proposed method to solve the optimization problem is shown in the flowchart in Figure 2:

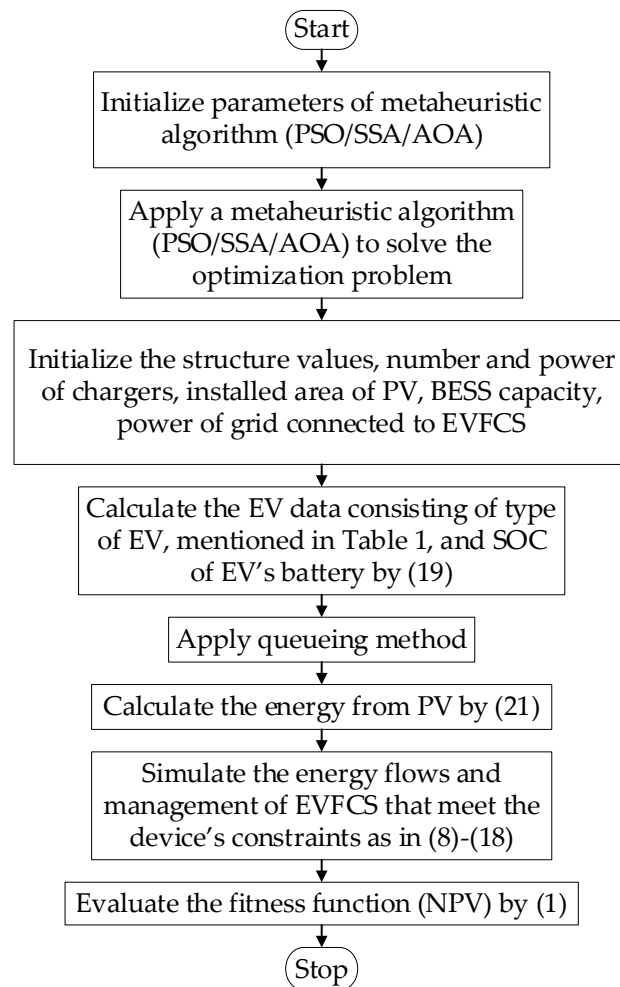


**Figure 2.** Flowchart of the proposed method for solving the optimal design of the EVFCS problem.

## 5. Simulation Results

This work aims to find the optimal structure of the EVFCS in order to maximize the NPV. The simulation was operated in MATLAB, and the computer specification was an Intel Core i7, RAM 16 GB. The input data and parameters for the system model are explained in this section. The simulation results consisting of the queuing of EV and EV demands are presented. PSO, SSA, and AOA were applied to solve the optimization problem and to find the optimal energy flows and management within the EVFCS, and the results obtained from these algorithms were compared. In addition, since this work considers the optimal design of the EVFCS, the EVFCS is assumed to be optimally placed in one station. The energy is also assumed to flow within a station or the energy does not flow into any bus, so power loss has not been considered in this work.

### 5.1. Input System Data

The data used to simulate the metaheuristic algorithms for solving the problem can be found in this subsection. The limits of the system variables which are also used to initialize the positions of the metaheuristic algorithms are presented in Table 2 [2], and the charging power levels of chargers are shown in Table 3 [47–49] to ensure that the charger power limits used in this work in Table 2 are within the range of the fast charger. The economic parameters are presented in Table 4. The parameters in Table 4 are the values used in the Spanish system and the electricity market of Spain [2], and these are adopted to evaluate the NPV in this work. Additionally, the purchase and sale prices of energy to the grid and the energy sale price to EVs are fixed throughout the year [2,11]. The minimum SOC level

of BESS is 10% or 0.1 p.u, and its life cycle is 2000 cycles, and the cost of maintaining BESS is set to be constant throughout the year [2]. Finally, the time of the cash flow and interest rate are 20 years and 2.69%, respectively [2,6].

**Table 2.** Limits of optimization variables.

Variable	Type	Lower Bound	Upper Bound
Number of chargers: $Q_{ch}$	Integer	1	10
Charger power (kW): $P_{ch_{inst}}$	Integer	44	220
Installed photovoltaic panels area (m <sup>2</sup> ): $Apv_{inst}$	Real	0	1875
Battery capacity (kWh): $Esto_{inst}$	Real	0	500
Maximum grid power connected to the EVFCS (kW): $P_{gc_{max}}$	Real	0	600

**Table 3.** Charging power levels.

Power Level Type	Maximum Power (kW)	Standard
Level 1 (Slow) [47,49]	1.4–3.7	SAE J1772 (Type 1)
Level 2 (Slow) [47]	3.7–43.5	IEC 62196 (Type 2), SAE J1772 (Type 1), SAE J3068
Level 3 (Fast) [48]	50	CHAdeMoO 1.0
	120	GB/T
	150	SAE Combo-1, CHAdemo 1.0
	200	CCS Combo 2
	350	SAE Combo-1, CHAdemo 1.2

**Table 4.** Economic costs for evaluating NPV.

Parameter	Price
PV panels	118.110 \$/m <sup>2</sup>
EV charger	590.550 \$/kW
BESS (Li-ion)	177.165 \$/kWh
BESS maintenance	1181.100 \$/year
Sell energy to EV	0.207 \$/kWh
Sell energy to Grid	0.065 \$/kWh
Buy energy from grid	0.159 \$/kWh
Contracted power to grid	0.142 \$/kW/month

## 5.2. Results

In this subsection, the optimal structural design of the EVFCS is simulated, and the simulation results consisting of the EV demands, the queuing of EVs, and the energy flows and management are presented. Then, the optimal station's structure configuration and economic aspects are obtained by using three optimization algorithms, which are PSO, SSA, and AOA.

### 5.2.1. EV Demands

The battery capacity and SOC of the EV's battery are simulated for each EV by using (19) and the data from Table 1. Then, the simulation results are used to calculate the energy needed to fill the battery of EVs. The results of the simulation of the EV demands are shown in Figure 3.

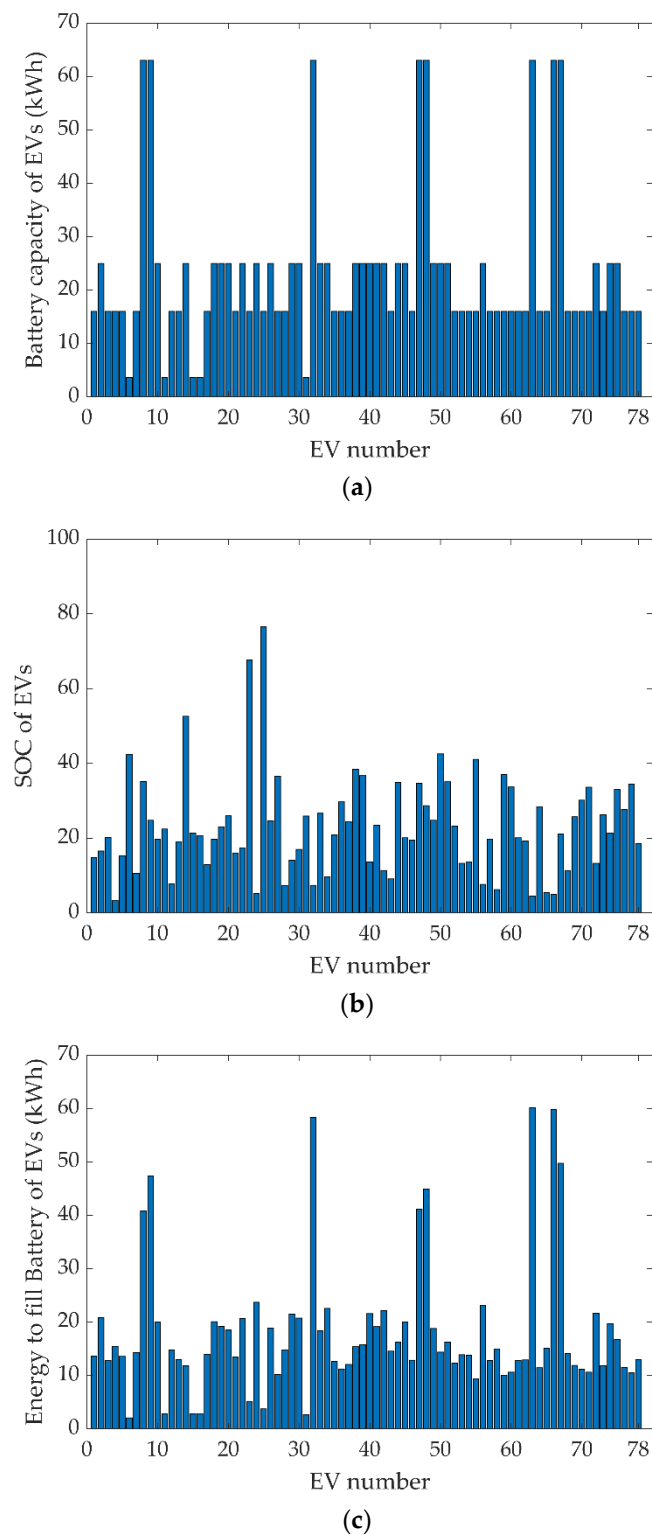


**Figure 3.** EV demand simulation results: (a) battery capacity of each EV; (b) SOC level of each EV's battery; (c) energy to fill the battery of each EV.

In this subsection, the battery capacity and SOC level of each EV are obtained, and these results are calculated to find the energy to charge the battery of each EV. Then, the EVs are allocated to the chargers (queuing of EVs) that can be found in the next subsection.

### 5.2.2. Queuing of EVs

The queuing method of EVs is explained in this subsection. Firstly, EVs that arrive at the EVFCS during a day are divided into 3 periods in an hour (20 min per period) because the charging time of each EV is defined as not more than 20 min in this work. Then, the EVs are allocated to the chargers, and if EV customers arrive at the station and the chargers are unavailable, customers then immediately leave the station. The number of EVs arriving at the EVFCS in each period is presented in Figure 4. For example, if the EVFCS comprises 4 chargers, the queuing of the EVs to these chargers can be presented in Figure 5.

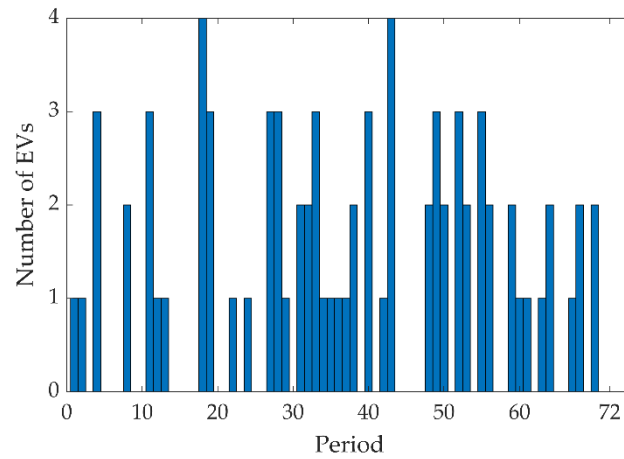


Figure 4. Number of EVs arriving at the EVFCS in each period.

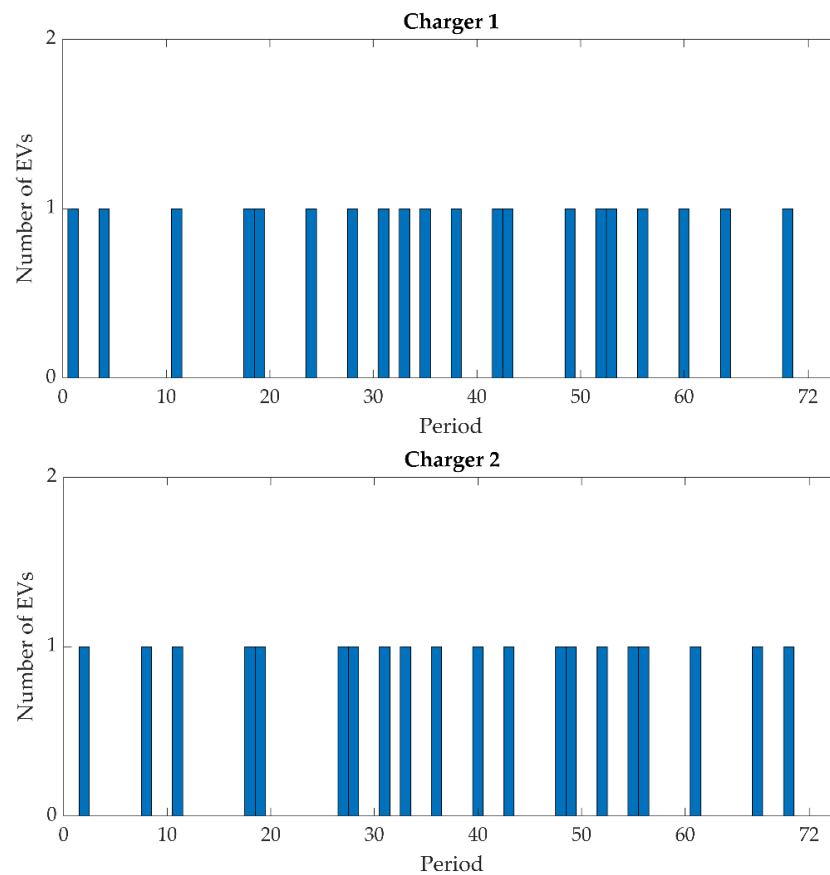
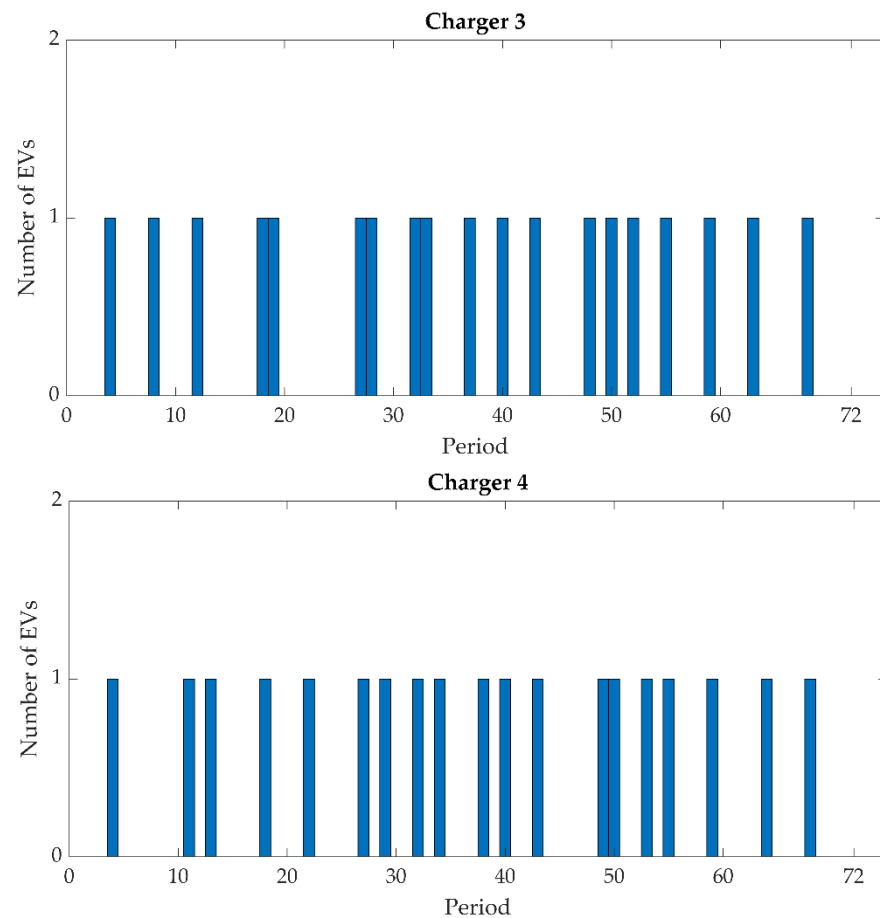


Figure 5. Cont.





**Figure 5.** Number of EVs at each charger.

Then, the hourly global solar irradiance calculated by (21) is obtained as in Figure 6 to find the hourly power generated by the PV panels.

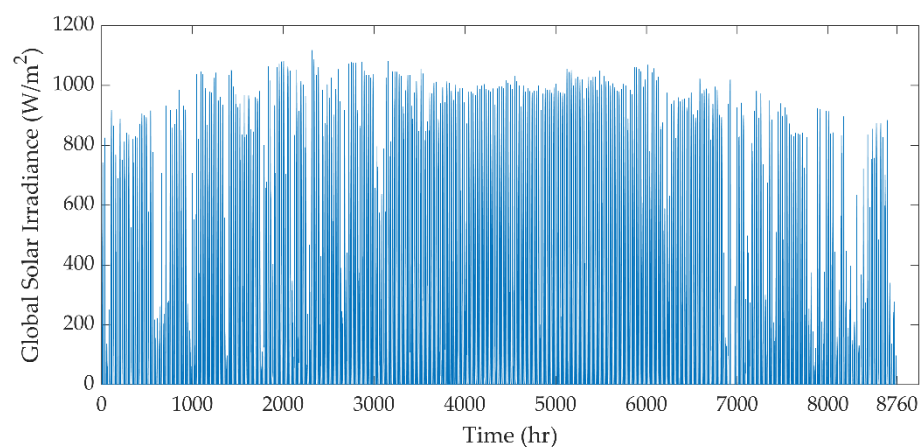


**Figure 6.** Hourly global solar irradiance.

The number of EVs allocated to the chargers in each period provided by the queueing method in this subsection and the energy fed into the battery of each EV obtained from Section 5.2.1 are used to calculate the energy charged to EVs in each hour ( $E_{ev_h}$ ). In addition, the hourly global solar irradiance in Figure 6 is adopted to obtain the hourly power generated by the PV panels. Then, the energy charged to EVs in each hour and the

hourly power generated by the PV panels are applied to calculate the energy flows in the EVFCS as presented in the next subsection.

### 5.2.3. Performance Comparison of the Optimization Algorithms

The optimal solutions of the EVFCS design obtained by the considered metaheuristic algorithms are presented in terms of the station’s structure configuration and economic aspects. The optimal structures of the EVFCS provided by each algorithm are shown in Table 5. In this table, the installed number of chargers ( $Q_{ch}$ ), the installed power of chargers ( $P_{ch_{inst}}$ ), the installed area of PV panels ( $A_{pv_{inst}}$ ), the installed BESS capacity ( $E_{sto_{inst}}$ ), the maximum grid power connected to the EVFCS ( $P_{gc_{max}}$ ), and the computational time are presented. The energy flows and management of the EVFCS over the course of a year are simulated by using these optimization algorithms and presented as the daily energy flows and management of the EVFCS in Figure 7.

**Table 5.** Optimal structure of the EVFCS design generated by each algorithm.

Algorithm	$Q_{ch}$	$P_{ch_{inst}}$ (kW)	$A_{pv_{inst}}$ (m <sup>2</sup> )	$E_{sto_{inst}}$ (kWh)	$P_{gc_{max}}$ (kW)	Average Charging Time (min)	Computational Time (min)
PSO	4	71.04	1875.00	45.81	264.37	19.67	30.81
SSA	4	75.05	1833.56	136.48	289.79	18.95	31.64
AOA	4	80.73	1875.00	60.40	317.17	16.29	30.42

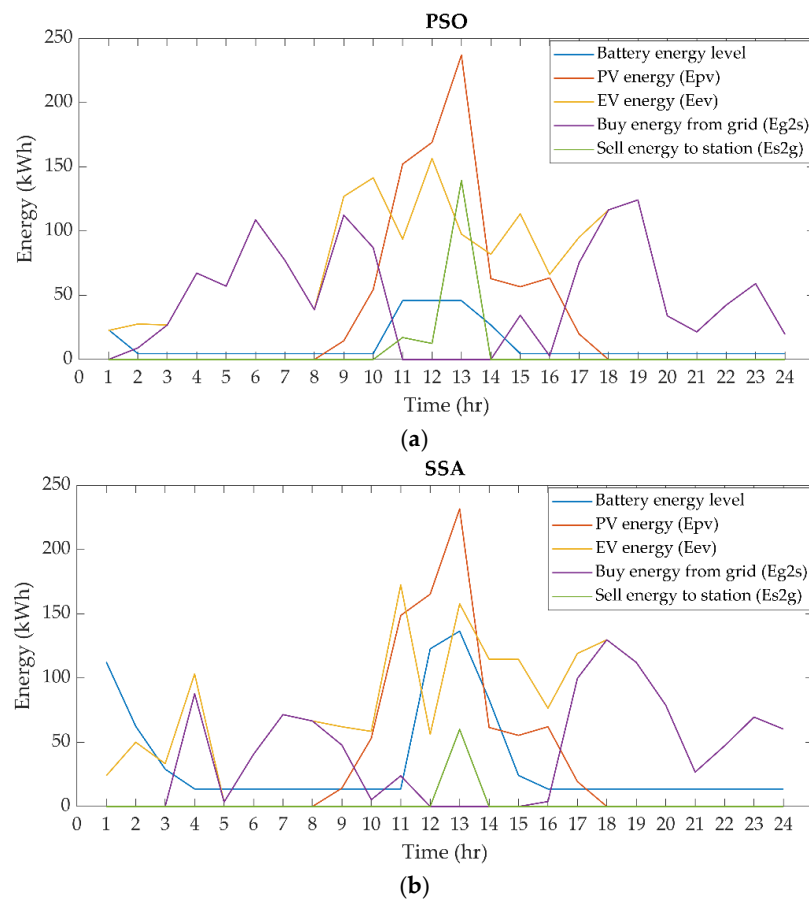


**Figure 7.** Cont.

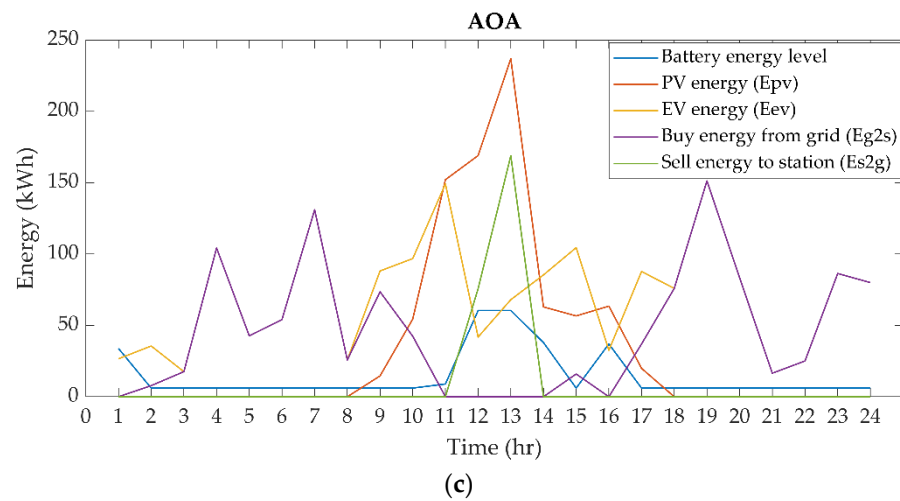


**Figure 7.** Daily energy flows and management of the EVFCS from each algorithm: (a) PSO; (b) SSA; (c) AOA.

From Table 5, the number of chargers obtained from all algorithms is 4. It can be seen from Table 5 and Figure 7 that AOA could achieve the highest power of chargers, followed by SSA and PSO which are 80.73 kW, 75.05 kW, and 71.04 kW, respectively, resulting in the average charging time of AOA being the lowest at 16.29 min. SSA provided the highest installed BESS capacity at 136.48 kWh, followed by AOA and PSO at 60.40 kWh and 45.81 kWh, respectively. The highest maximum grid power connected to the EVFCS obtained by AOA is 317.17 kW, while those of PSO and SSA are slightly different at 264.37 kW and 289.79 kW, respectively. The installed area of PV panels provided by PSO, SSA, and AOA are also slightly different at 1875.00 m<sup>2</sup>, 1833.56 m<sup>2</sup>, and 1875.00 m<sup>2</sup>, respectively.

The simulation results in the economic aspects during the cash flow time (20 years) provided by the considered metaheuristic algorithms are shown in Table 6. The NPV, investment cost, BESS replacement cost, maintenance cost, cost of buying energy from the grid, and cost of selling energy to the grid and EV customers are presented in this Table.

**Table 6.** Results in the economic aspects provided by each algorithm.

Algorithm	NPV (\$)	Investment Cost (\$)	Battery Replacement Cost (\$)	Maintenance Cost (\$/year)	Cost of Purchasing Energy from the Grid (\$/year)	Income from Selling Energy to the Grid (\$/year)	Income from Selling Energy to EV Customers (\$/year)
PSO	1,166,314.71	397,396.49	21,447.66	1181.10	50,530.37	18,661.20	137,020.93
SSA	1,132,487.00	418,042.90	59,157.77	1181.10	49,149.20	16,401.24	139,545.10
AOA	1,018,920.31	422,848.30	29,330.82	1181.10	53,670.53	22,461.30	129,003.00

From Table 6 and Figure 7, it is observed that PSO provided the best NPV at \$1,166,314.71, followed by SSA and AOA at \$1,132,487.00 and \$1,018,920.31 respectively. The investment cost from the PSO, SSA, and AOA are competitive at \$397,396.49, \$418,042.90, and \$422,848.30, respectively. SSA was found to have the highest BESS replacement cost at \$59,157.77/year because of the largest installed BESS size resulting in a higher cost than those of PSO and AOA, which are \$21,447.66/year and \$29,330.82/year, respectively. In addition, since the grid power connected to the EVFCS obtained by AOA is much greater than those of PSO and SSA, this results in the highest cost of buying energy from the grid at \$53,670.53/year, while the costs obtained by PSO and SSA are similar at \$50,530.37/year and \$49,149.20/year, respectively. However, AOA could generate the highest income from selling energy to the grid at \$22,461.30/year, followed by PSO which could generate \$18,661.20/year and SSA

at \$16,401.24/year. Finally, the incomes from selling energy to EVs given by PSO and SSA are slightly different at \$137,020.93/year and \$139,545.10/year respectively, while AOA may provide only \$129,003.00/year.

To further investigate the performance of the considered metaheuristic algorithms, the convergence curves of PSO, SSA, and AOA for solving the NPV objective are plotted in Figure 8, and the comparative analysis of the convergence characteristic of the proposed metaheuristic algorithm are presented in Table 7.

It can be noted from Figure 8 that PSO quickly converged to the feasible solution, followed by SSA and AOA. PSO also achieved the best NPV while SSA and AOA provided the second-best and third-best NPVs respectively. Further, Table 7 shows the verification of the performance of the considered metaheuristic algorithms. The maximum, minimum, and average values of NPV for each algorithm are provided in this table. By considering maximum, minimum, and average NPV values, PSO gives the best of all NPV values, followed by SSA and AOA, respectively.

Overall, in this work, the EV demands including the EV battery capacities, their SOC levels, and the queuing of EVs were obtained. Then, PSO, SSA, and AOA are used to find the optimal management of the energy flows in the EVFCS, along with the maximum NPV. It was found that PSO is the best algorithm to provide the optimal structure of the EVFCS configuration by considering the maximum NPV, while SSA is second-best, with competitive performance to PSO. AOA is the worst algorithm to find a solution that maximizes NPV. Consequently, PSO should be selected to design the optimal structure of the EVFCS to find a solution with the maximum NPV.

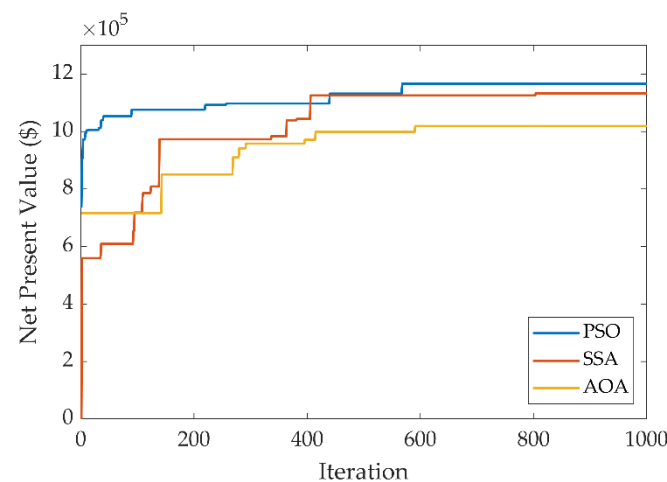


**Figure 8.** Convergence curves for each algorithm.

**Table 7.** Comparative analysis of the convergence characteristic of the proposed metaheuristic algorithm.

Algorithm	NPV (\$)		
	Max	Min	Average
PSO	1,166,314.71	1,093,304.50	1,129,809.60
SSA	1,132,487.00	980,483.30	1,056,485.15
AOA	1,018,920.31	870,332.16	944,626.23

## 6. Conclusions

In this work, the optimal design of the structure of EVFCS is presented. The EV demands consisting of the battery capacity and SOC of the EV's battery are simulated based on the probabilistic distribution, and the energy from PV is calculated by using realistic values. Moreover, this work has executed the simple EV queuing method where

EVs are allocated to the chargers, and if the EVs arrive at the station and the chargers are unavailable, EVs then leave the station. Three algorithms comprising PSO, SSA, and AOA are applied to find the optimal structure of the EVFCS and optimal management of the energy flows between PV, BESS, EVFCS, and the grid. Thus, the EVFCS can achieve the maximum profit determined by its NPV. In the simulation results, the energy charged to EVs in each hour is obtained by calculating the EV demands and using the queuing method. Three algorithms could determine the optimal energy flows within the EVFCS with the different obtained optimal structures and NPVs. The NPV results show that PSO is the best algorithm to give the optimal structure of the EVFCS, providing the highest NPV. Although SSA provides a rather different optimal structure of the EVFCS to PSO, SSA gives a very competitive NPV to that of PSO, while AOA proved the worst algorithm to achieve the maximum NPV. In conclusion, PSO and SSA are the best and second-best algorithms respectively for giving the optimal design of the EVFCS structure with the maximum NPV, while AOA is considered the worst algorithm.

In future work, the optimal design of the EVFCS will be considered in the IEEE distribution systems such as the IEEE 33-bus system, and power losses will be also considered. Several factors such as CO<sub>2</sub> emissions will be considered to enhance the design of the EVFCS in term of environmental improvement. In addition, more forms of renewable energy, such as wind turbines, can be considered in the future.

**Author Contributions:** Conceptualization, P.A. and S.K.; methodology, P.A. and S.K.; software, P.A.; validation, P.A., S.P., A.S. and S.K.; formal analysis, P.A. and S.K.; investigation, P.A. and S.K.; resources, P.A.; data curation, P.A.; writing—original draft preparation, P.A. and S.K.; writing—review and editing, P.A., S.P., A.S. and S.K.; visualization, P.A. and S.K.; supervision, S.P., A.S. and S.K.; project administration, S.P., A.S. and S.K.; funding acquisition, S.K. All authors have read and agreed to the published version of the manuscript.

**Funding:** This research was funded by the Teaching Assistant and Research Assistant (TA/RA) Scholarship from the Graduate School, Chiang Mai University.

**Institutional Review Board Statement:** Not applicable.

**Informed Consent Statement:** Not applicable.

**Data Availability Statement:** Not applicable.

**Acknowledgments:** The authors have received the Teaching Assistant and Research Assistant (TA/RA) Scholarship from the Graduate School, Chiang Mai University.

**Conflicts of Interest:** The authors declare no conflict of interest.

## Abbreviations

ATP	arrival time-based priority algorithm
AOA	arithmetic optimization algorithm
BESS	battery energy storage systems
BN	Bayesian network
BFOA-PSO	hybrid bacterial foraging optimization algorithm and particle swarm optimization
CSO	chicken swarm optimization
CSA	cuckoo search algorithm
EVs	electric vehicles
EVCS	electric vehicle charging stations
EVFCS	electric vehicle fast-charging station
ESS	energy storage system
GA-BPSO	genetic algorithm with binary particle swarm optimization
GA	genetic algorithm
IHOGA	improved hybrid optimization genetic algorithm
MINLP	mixed-integer non-linear programming
MCMP	multiple-charger multiple-port charging

MAPSO	multi-agent particle swarm optimization algorithm
NPV	net present value
PSO	particle swarm optimization
PV	photovoltaic
PVGIS	photovoltaic geographical information system
SOC	state of charge
SPB	state of charge-based priority algorithm
SFLA	shuffled frog leaping algorithm
SAA	simulated annealing algorithm
SSA	Salp swarm algorithm
SMC	Sequential Monte Carlo
TLBO	teaching-learning-based optimization
WT	wind turbine

## References

1. Sadeghi-Barzani, P.; Rajabi-Ghahnavieh, A.; Kazemi-Karegar, H. Optimal Fast Charging Station Placing and Sizing. *Appl. Energy* **2014**, *125*, 289–299. [[CrossRef](#)]
2. Domínguez-Navarro, J.A.; Dufo-López, R.; Yusta-Loyo, J.M.; Artal-Sevil, J.S.; Bernal-Agustín, J.L. Design of an Electric Vehicle Fast-Charging Station with Integration of Renewable Energy and Storage Systems. *Int. J. Electr. Power Energy Syst.* **2019**, *105*, 46–58. [[CrossRef](#)]
3. Ahmad, F.; Khalid, M.; Panigrahi, B.K. An Enhanced Approach to Optimally Place the Solar Powered Electric Vehicle Charging Station in Distribution Network. *J. Energy Storage* **2021**, *42*, 103090. [[CrossRef](#)]
4. Tounsi Fokui, W.S.; Saulo, M.J.; Ngoo, L. Optimal Placement of Electric Vehicle Charging Stations in a Distribution Network with Randomly Distributed Rooftop Photovoltaic Systems. *IEEE Access* **2021**, *9*, 132397–132411. [[CrossRef](#)]
5. Yenhamchalit, K.; Kongjeen, Y.; Prabpal, P.; Bhummkittipich, K. Optimal Placement of Distributed Photovoltaic Systems and Electric Vehicle Charging Stations Using Metaheuristic Optimization Techniques. *Symmetry* **2021**, *13*, 2378. [[CrossRef](#)]
6. Vermaak, H.J.; Kusakana, K. Design of a Photovoltaic-Wind Charging Station for Small Electric Tuk-Tuk in D.R.Congo. *Renew Energy* **2014**, *67*, 40–45. [[CrossRef](#)]
7. Hafez, O.; Bhattacharya, K. Optimal Design of Electric Vehicle Charging Stations Considering Various Energy Resources. *Renew Energy* **2017**, *107*, 576–589. [[CrossRef](#)]
8. Hussain, A.; Bui, V.H.; Kim, H.M. Optimal Sizing of Battery Energy Storage System in a Fast EV Charging Station Considering Power Outages. *IEEE Trans. Transp. Electrification* **2020**, *6*, 453–463. [[CrossRef](#)]
9. Dai, Q.; Liu, J.; Wei, Q. Optimal Photovoltaic/Battery Energy Storage/Electric Vehicle Charging Station Design Based Onmulti-Agent Particle Swarm Optimization Algorithm. *Sustainability* **2019**, *11*, 1973. [[CrossRef](#)]
10. Badea, G.; Felseghi, R.A.; Varlam, M.; Filote, C.; Culcer, M.; Iliescu, M.; Raboaca, M.S. Design and Simulation of Romanian Solar Energy Charging Station for Electric Vehicles. *Energies* **2019**, *12*, 74. [[CrossRef](#)]
11. Bhatti, A.R.; Salam, Z.; Sultana, B.; Rasheed, N.; Awan, A.B.; Sultana, U.; Younas, M. Optimized Sizing of Photovoltaic Grid-Connected Electric Vehicle Charging System Using Particle Swarm Optimization. *Int. J. Energy Res.* **2019**, *43*, 500–522. [[CrossRef](#)]
12. Zhang, Y.; You, P.; Cai, L. Optimal Charging Scheduling by Pricing for EV Charging Station with Dual Charging Modes. *IEEE Trans. Intell. Transp. Syst.* **2019**, *20*, 3386–3396. [[CrossRef](#)]
13. Savari, G.F.; Krishnasamy, V.; Guerrero, J.M. Optimal Scheduling and Economic Analysis of Hybrid Electric Vehicles in a Microgrid. *Int. J. Emerg. Electr. Power Syst.* **2018**, *19*. [[CrossRef](#)]
14. Abbas, F.; Feng, D.; Habib, S.; Numan, M.; Rahman, U. A Heuristically Optimized Comprehensive Charging Scheme for Large-Scale EV Integration. *Int. Trans. Electr. Energy Syst.* **2020**, *30*, e12313. [[CrossRef](#)]
15. Hou, W.; Luo, Q.; Wu, X.; Zhou, Y.; Si, G. Multiobjective Optimization of Large-Scale EVs Charging Path Planning and Charging Pricing Strategy for Charging Station. *Complexity* **2021**, *2021*, 8868617. [[CrossRef](#)]
16. Savari, G.F.; Krishnasamy, V.; Sugavanam, V.; Vakesan, K. Optimal Charging Scheduling of Electric Vehicles in Micro Grids Using Priority Algorithms and Particle Swarm Optimization. *Mob. Netw. Appl.* **2019**, *24*, 1835–1847. [[CrossRef](#)]
17. Leou, R.C.; Hung, J.J. Optimal Charging Schedule Planning and Economic Analysis for Electric Bus Charging Stations. *Energies* **2017**, *10*, 483. [[CrossRef](#)]
18. Shaaban, M.F.; Eajal, A.A.; El-Saadany, E.F. Coordinated Charging of Plug-in Hybrid Electric Vehicles in Smart Hybrid AC/DC Distribution Systems. *Renew Energy* **2015**, *82*, 92–99. [[CrossRef](#)]
19. Erdinc, O.; Tascikaraoglu, A.; Paterakis, N.G.; Dursun, I.; Sinim, M.C.; Catalao, J.P.S. Comprehensive Optimization Model for Sizing and Siting of DG Units, EV Charging Stations, and Energy Storage Systems. *IEEE Trans. Smart Grid* **2018**, *9*, 3871–3882. [[CrossRef](#)]
20. Hosseini, S.; Sarder, M.D. Development of a Bayesian Network Model for Optimal Site Selection of Electric Vehicle Charging Station. *Int. J. Electr. Power Energy Syst.* **2019**, *105*, 110–122. [[CrossRef](#)]
21. Hu, D.; Zhang, J.; Zhang, Q. Optimization Design of Electric Vehicle Charging Stations Based on the Forecasting Data with Service Balance Consideration. *Appl. Soft Comput. J.* **2019**, *75*, 215–226. [[CrossRef](#)]



22. Khalid, M.; Ahmad, F.; Panigrahi, B.K.; Al-Fagih, L. A Comprehensive Review on Advanced Charging Topologies and Methodologies for Electric Vehicle Battery. *J. Energy Storage* **2022**, *53*, 105084. [[CrossRef](#)]
23. Khalid, M.; Ahmad, F.; Panigrahi, B.K. Design, Simulation and Analysis of a Fast Charging Station for Electric Vehicles. *Energy Storage* **2021**, *3*, e263. [[CrossRef](#)]
24. Khalid, M.; Ahmad, F.; Panigrahi, B.K.; Rahman, H. A Capacity Efficient Power Distribution Network Supported by Battery Swapping Station. *Int. J. Energy Res.* **2022**, *46*, 4879–4894. [[CrossRef](#)]
25. Stojkovic, J. Multi-Objective Optimal Charging Control of Electric Vehicles in PV Charging Station. *IEEE Power Energy Soc.* **2019**. [[CrossRef](#)]
26. Chen, H.; Hu, Z.; Luo, H.; Qin, J.; Rajagopal, R.; Zhang, H. Design and Planning of a Multiple-Charger Multiple-Port Charging System for PEV Charging Station. *IEEE Trans. Smart Grid* **2019**, *10*, 173–183. [[CrossRef](#)]
27. Savio, D.A.; Juliet, V.A.; Chokkalingam, B.; Padmanaban, S.; Holm-Nielsen, J.B.; Blaabjerg, F. Photovoltaic Integrated Hybrid Microgrid Structured Electric Vehicle Charging Station and Its Energy Management Approach. *Energies* **2019**, *12*, 168. [[CrossRef](#)]
28. del Valle, Y.; Venayagamoorthy, G.K.; Mohagheghi, S.; Hernandez, J.-C.; Harley, R.G. Particle Swarm Optimization: Basic Concepts, Variants and Applications in Power Systems. *IEEE Trans. Evol. Comput.* **2008**, *12*, 171–195. [[CrossRef](#)]
29. Mirjalili, S.; Gandomi, A.H.; Mirjalili, S.Z.; Saremi, S.; Faris, H.; Mirjalili, S.M. Salp Swarm Algorithm: A Bio-Inspired Optimizer for Engineering Design Problems. *Adv. Eng. Softw.* **2017**, *114*, 163–191. [[CrossRef](#)]
30. Abualigah, L.; Diabat, A.; Mirjalili, S.; Abd Elaziz, M.; Gandomi, A.H. The Arithmetic Optimization Algorithm. *Comput. Methods Appl. Mech. Eng.* **2021**, *376*, 113609. [[CrossRef](#)]
31. Eltamaly, A.M.; Al-Saud, M.S.; Abo-Khalil, A.G. Performance Improvement of PV Systems' Maximum Power Point Tracker Based on a Scanning PSO Particle Strategy. *Sustainability* **2020**, *12*, 1185. [[CrossRef](#)]
32. Chamchuen, S.; Siritariwat, A.; Fuangfoo, P.; Suthisopapan, P.; Khunkitti, P. High-Accuracy Power Quality Disturbance Classification Using the Adaptive ABC-PSO as Optimal Feature Selection Algorithm. *Energies* **2021**, *14*, 1238. [[CrossRef](#)]
33. Eltamaly, A.M. A Novel Strategy for Optimal Pso Control Parameters Determination for Pv Energy Systems. *Sustainability* **2021**, *13*, 1008. [[CrossRef](#)]
34. Khaboot, N.; Srihapon, C.; Siritariwat, A.; Khunkitti, P. Increasing Benefits in High PV Penetration Distribution System by Using Battery Energy Storage and Capacitor Placement Based on Salp Swarm Algorithm. *Energies* **2019**, *12*, 4817. [[CrossRef](#)]
35. Aprillia, H.; Yang, H.T.; Huang, C.M. Short-Term Photovoltaic Power Forecasting Using a Convolutional Neural Network-Salp Swarm Algorithm. *Energies* **2020**, *13*, 1879. [[CrossRef](#)]
36. Mahmoud, K.; Abdel-Nasser, M.; Mustafa, E.; Ali, Z.M. Improved Salp-Swarm Optimizer and Accurate Forecasting Model for Dynamic Economic Dispatch in Sustainable Power Systems. *Sustainability* **2020**, *12*, 576. [[CrossRef](#)]
37. Abualigah, L.; Diabat, A.; Sumari, P.; Gandomi, A.H. A Novel Evolutionary Arithmetic Optimization Algorithm for Multilevel Thresholding Segmentation of COVID-19 Ct Images. *Processes* **2021**, *9*, 1155. [[CrossRef](#)]
38. Khatir, S.; Tiachacht, S.; le Thanh, C.; Ghandourah, E.; Mirjalili, S.; Abdel Wahab, M. An Improved Artificial Neural Network Using Arithmetic Optimization Algorithm for Damage Assessment in FGM Composite Plates. *Compos. Struct.* **2021**, *273*, 114287. [[CrossRef](#)]
39. Zhang, P.; Qian, K.; Zhou, C.; Stewart, B.G.; Hepburn, D.M. A Methodology for Optimization of Power Systems Demand Due to Electric Vehicle Charging Load. *IEEE Trans. Power Syst.* **2012**, *27*, 1628–1636. [[CrossRef](#)]
40. Fazelpour, F.; Vafaeipour, M.; Rahbari, O.; Shirmohammadi, R. Considerable Parameters of Using PV Cells for Solar-Powered Aircrafts. *Renew. Sustain. Energy Rev.* **2013**, *22*, 81–91. [[CrossRef](#)]
41. Photovoltaic Geographical Information System (PVGIS) | EU Science Hub. Available online: <https://ec.europa.eu/jrc/en/pvgis> (accessed on 13 December 2021).
42. Benavides, D.; Arévalo, P.; Tostado-Véliz, M.; Vera, D.; Escamez, A.; Aguado, J.A.; Jurado, F. An Experimental Study of Power Smoothing Methods to Reduce Renewable Sources Fluctuations Using Supercapacitors and Lithium-Ion Batteries. *Batteries* **2022**, *8*, 228. [[CrossRef](#)]
43. Hossain Lipu, M.S.; Miah, M.S.; Ansari, S.; Wali, S.B.; Jamal, T.; Elavarasan, R.M.; Kumar, S.; Naushad Ali, M.M.; Sarker, M.R.; Aljanad, A.; et al. Smart Battery Management Technology in Electric Vehicle Applications: Analytical and Technical Assessment toward Emerging Future Directions. *Batteries* **2022**, *8*, 219. [[CrossRef](#)]
44. Fathabadi, H. Novel Stand-Alone, Completely Autonomous and Renewable Energy Based Charging Station for Charging Plug-in Hybrid Electric Vehicles (PHEVs). *Appl. Energy* **2020**, *260*, 114194. [[CrossRef](#)]
45. Lipu, M.S.H.; Al Mamun, A.; Ansari, S.; Miah, M.S.; Hasan, K.; Meraj, S.T.; Abdolrasol, M.G.M.; Rahman, T.; Maruf, M.H.; Sarker, M.R.; et al. Battery Management, Key Technologies, Methods, Issues, and Future Trends of Electric Vehicles: A Pathway toward Achieving Sustainable Development Goals. *Batteries* **2022**, *8*, 119. [[CrossRef](#)]
46. Khunkitti, S.; Siritariwat, A.; Premrudeepreechacharn, S.; Chatthaworn, R.; Watson, N.R. A Hybrid DA-PSO Optimization Algorithm for Multiobjective Optimal Power Flow Problems. *Energies* **2018**, *11*, 2270. [[CrossRef](#)]
47. Khalid, M.R.; Khan, I.A.; Hameed, S.; Asghar, M.S.J.; Ro, J.S. A Comprehensive Review on Structural Topologies, Power Levels, Energy Storage Systems, and Standards for Electric Vehicle Charging Stations and Their Impacts on Grid. *IEEE Access* **2021**, *9*, 128069–128094. [[CrossRef](#)]

48. Tu, H.; Feng, H.; Srdic, S.; Lukic, S. Extreme Fast Charging of Electric Vehicles: A Technology Overview. *IEEE Trans. Transp. Electrification* **2019**, *5*, 861–878. [[CrossRef](#)]
49. Ronanki, D.; Kelkar, A.; Williamson, S.S. Extreme Fast Charging Technology—Prospects to Enhance Sustainable Electric Transportation. *Energies* **2019**, *12*, 3721. [[CrossRef](#)]

**Disclaimer/Publisher’s Note:** The statements, opinions and data contained in all publications are solely those of the individual author(s) and contributor(s) and not of MDPI and/or the editor(s). MDPI and/or the editor(s) disclaim responsibility for any injury to people or property resulting from any ideas, methods, instructions or products referred to in the content.